IAES International Journal of Robotics and Automation (IJRA)
Vol. 15, No. 4, December 2026, pp. 987~1000
ISSN: 2722-2586, DOI: 10.11591/ijra.v15i4.pp987-1000

Design and performance analysis of an IoT-based vehicle exhaust emission monitoring system using ESP32 and MQ gas sensors

Nuraeni Umar[1], Riesa Krisna Astuti Sakir[1], Muhira Dzar Faraby[1], Sufianti Munirman[1], Asma Amaliah[1], Andi Mutiah Nurul Aini[1], Latifah Wulandari[1], Nurhayati[2], Yuli Asmi Rahman[3], Andi Nur Putri[4]

[1]Department of Electrical and Computer Engineering, State Polytechnic of Ujung Pandang, Makassar, Indonesia
[2]Department of Multimedia and Network Engineering, State Polytechnic of Ujung Pandang, Makassar, Indonesia
[3]Department of Electrical Engineering, University of Tadulako, Palu, Indonesia
[4]Department of Electrical Engineering, University of Patria Artha, Gowa, Indonesia

Article Info

Article history:

Received Jun 15, 2026
Revised Oct 1, 2026
Accepted Nov 10, 2026

Keywords:

Carbon monoxide detection
ESP32
Internet of Things
MQ gas sensors
Vehicle emission monitoring

ABSTRACT

This study develops and evaluates an automated vehicle exhaust monitoring and decision-support system based on an ESP32 microcontroller and low-cost MQ-series gas sensors. The system automatically acquires sensor responses, estimates exhaust-gas concentrations, evaluates predefined emission-response levels, activates visual and audible alerts, and transmits monitoring data to a cloud platform without continuous manual intervention. Experimental evaluation was conducted using motorcycles and automobiles manufactured between 1978 and 2023. Comparison with a standardized automotive exhaust gas analyzer showed pointwise differences ranging from approximately 0.01 to 0.13 percentage points for CO and 0.1 to 0.5 percentage points for the reported CO_2-related values under the selected test conditions. These results demonstrate the feasibility of the proposed architecture for preliminary automated emission screening, while limitations related to sensor operating range, cross-sensitivity, and calibration uncertainty indicate the need for further controlled validation. Overall, the proposed system functioned effectively as a preliminary emission monitoring solution, although additional sensor calibration and hardware improvements are necessary to enhance measurement accuracy, consistency, and long-term reliability.

This is an open access article under the CC BY-SA license.

Corresponding Author:

Nuraeni Umar
Department of Electrical Engineering, Ujung Pandang State Polytecnic
St. Perintis Kemerdekaan Km. 10 Tamalanrea, Makassar 90245, Indonesia
Email: nuraeni_umar@poliupg.ac.id

1. INTRODUCTION

Air pollution continues to be a major environmental and health concern worldwide. According to the World Health Organization (WHO), nearly 90% of the global population is exposed to air quality levels that exceed recommended standards [1]. This condition is associated with approximately 7.9 million premature deaths each year, with around 86% of cases related to noncommunicable diseases, including cardiovascular disorders, chronic obstructive pulmonary disease (COPD), stroke, and lung cancer [2], [3]. In Indonesia, the transportation sector represents the second-largest contributor to greenhouse gas (GHG) emissions, where road transportation contributes nearly 90% of the sector's total emissions [4]. Data from 2022 indicate that land transportation produced about 110 million tons of CO_2, largely influenced by the

dominance of motorcycles, which accounted for 84.54% of the nation's registered vehicles [5]. Furthermore, projections suggest that, without effective mitigation measures and policy implementation, emissions from urban road transport may increase up to 65-fold by 2050 [6]. Such growth is expected to worsen the accumulation of pollutants, including carbon monoxide (CO), nitrogen oxides (NO_x), and fine particulate matter ($PM_{2.5}$), particularly in highly populated metropolitan areas such as Jakarta [7].

Vehicle exhaust emissions, particularly carbon monoxide (CO) and carbon dioxide (CO_2), represent significant risks to both human health and environmental quality. Carbon monoxide is a highly toxic gas that binds to hemoglobin with an affinity nearly 200 times greater than oxygen, reducing the blood's oxygen-carrying capacity and potentially causing symptoms such as headaches, dizziness, fatigue, loss of consciousness, and even death at high concentrations [8]. Long-term exposure to lower levels of CO has also been associated with cardiovascular disorders, neurological impairment, and respiratory diseases [9]. These health risks are often intensified in developing countries such as Indonesia, where older and inadequately maintained vehicles tend to produce higher CO emissions due to incomplete combustion and declining catalytic converter performance. Beyond its impact on human health, vehicle-generated CO and CO_2 contribute to environmental problems, including tropospheric ozone formation and global warming, making emission reduction an important aspect of climate mitigation efforts and environmental policies [10]. However, conventional vehicle emission testing systems are generally expensive, stationary, and limited to designated inspection facilities, restricting their ability to provide continuous monitoring. The Internet of Things (IoT) offers an effective alternative by enabling portable and interconnected monitoring systems that combine gas sensors, embedded microcontrollers, and cloud-based technologies for real-time data acquisition and analysis [11]. Low-cost sensors such as the MQ-7 and MQ-135, integrated with Wi-Fi-enabled ESP32 microcontrollers, provide an affordable solution for emission monitoring, particularly in resource-constrained environments [12]–[14]. In addition, cloud platforms such as Blynk and ThingSpeak facilitate remote access, visualization, and management of monitoring data, supporting their implementation within smart city and intelligent transportation ecosystems [13].

Previous research has explored the application of IoT technology for air quality and vehicle emission monitoring through various approaches, such as ESP32-based multi-sensor systems integrated with ThingSpeak for data visualization [12], real-time environmental monitoring frameworks utilizing IoT technologies [11], Blynk-supported platforms that enable remote monitoring through smartphones [13], [14], and air quality monitoring systems employing MQ-series gas sensors for detection and purification purposes [15]–[17]. Comparison of the proposed automated vehicle-emission monitoring system can be seen in Table 1.

Table 1. Comparison of the proposed automated vehicle-emission system

Study	Sensors	Platform and Communication	Automated/Remote Functions	Validation/Reported Performance	Main Limitation
Easterline *et al.* [12]	MQ-2, MQ-7, MQ-8, MQ-135, DHT11	NodeMCU ESP32; Wi-Fi / ThingSpeak	Cloud visualization and local display	Ambient air monitoring; gas-sensor accuracy and latency not reported	No vehicle-exhaust analyzer validation
Farrag *et al.* [18]	Multi-gas sensors for CO, CO_2, NO, NO_2, H_2S, HC, and O_2	ESP32-S3; Wi-Fi, BLE, CAN/OBD-II	Fuzzy classification, notification, prediction, web dashboard	Prediction accuracy 83%; F1-score 0.79; real-world evaluation	More complex and relatively costly architecture
Priya *et al.* [19]	MQ-7, MiCS-5524, TGS2600, PMS5003	Edge computing, XGBoost, blockchain	Automated monitoring, prediction, and remote monitoring	Prediction accuracy 97.98%; response time 91.98 ms	Mainly evaluates ML/blockchain performance rather than gas-sensor accuracy
Proposed system	MQ-7 and MQ-135	ESP32; Wi-Fi / Blynk IoT	Automatic acquisition, classification, LED/buzzer alerts, local and cloud monitoring	Tested on 10 vehicles; 6 compared with reference analyzer; ΔCO = 0.01–0.13 percentage points and ΔCO_2 = 0.1–0.5 percentage points	Limited sensor range, cross-sensitivity, small sample, and no systematic latency/power evaluation

Despite these advancements, several limitations remain. Many existing systems do not provide multi-level audio-visual Level 2 features, lack comprehensive validation against standardized emission measurement instruments, and rarely evaluate emission characteristics across vehicles with different manufacturing years and engine technologies. In addition, few studies combine local real-time display with cloud-based remote monitoring within a single integrated platform. To overcome these shortcomings, this study develops an IoT-based vehicle exhaust emission monitoring system that integrates an ESP32 microcontroller [12], MQ-7 and MQ-135 gas sensors [12], [17], an OLED display, LED indicators, a buzzer-

based Level 2 system, and the Blynk IoT platform for real-time remote access and monitoring [13]. To address these limitations, this study investigates the practical application of low-cost MQ-series MOS sensors for preliminary vehicle exhaust monitoring under direct exhaust conditions. The main contributions of this work are the characterization of MQ-7 and MQ-135 sensor responses across vehicles of different manufacturing years and engine technologies, implementation of sensor-response processing and calibration procedures, and comparison of the resulting estimates with a standardized automotive exhaust gas analyzer. Particular attention is also given to the practical limitations of low-cost MOS sensors, including restricted operating ranges, cross-sensitivity, calibration uncertainty, and performance under high-concentration exhaust conditions. The OLED display, LED indicators, buzzer, and Blynk platform are employed as supporting features for local visualization, notification, and remote monitoring rather than as the primary scientific contribution. To address these limitations, this study develops an automated vehicle-emission monitoring and decision-support architecture in which sensing, data acquisition, sensor-response processing, emission-response classification, alert generation, and cloud transmission are performed automatically by an ESP32-based controller. The contribution of the work lies not in the individual use of common IoT components, but in their integration into an automated monitoring workflow combined with experimental characterization and preliminary validation of low-cost MOS sensor responses under vehicle-exhaust conditions. Particular attention is given to sensor operating-range limitations, cross-sensitivity, calibration uncertainty, and practical deployment in high-concentration exhaust environments.

The experimental results show that older vehicles produce higher CO and CO_2 emissions than newer models due to reduced combustion efficiency, engine wear, and aging-related degradation [6], [9]. This finding is consistent with previous studies linking vehicle age to increased emissions. The proposed system also demonstrated satisfactory performance for preliminary emission assessment and potential use in environmental and smart transportation monitoring [11]. The remainder of this paper is organized as follows: Section 2 reviews related studies, Section 3 describes the system design and implementation, Section 4 presents the experiments and results, Section 5 discusses system performance and validation, and Section 6 concludes the study and suggests future improvements.

2. RESEARCH METHOD

2.1. System overview

The developed system is an IoT-enabled vehicle exhaust emission monitoring platform designed to measure, analyze, and transmit carbon monoxide (CO) and carbon dioxide (CO_2) concentration data in real time. Its architecture is based on the three-layer IoT framework [11], consisting of a sensing layer, a processing layer, and a communication layer. The sensing layer employs MQ-7 and MQ-135 metal-oxide semiconductor (MOS) sensors to detect exhaust gas concentrations [12], [18]. The processing and alert layer is centered on an ESP32 microcontroller, which manages data acquisition, processing, and local notifications through an OLED display, LED indicators, and a buzzer [18]. Meanwhile, the communication layer utilizes the Blynk IoT platform to enable wireless data transmission and remote monitoring through internet-connected devices [13]. By combining portability, affordability, and real-time connectivity, the proposed system offers an alternative to conventional emission testing equipment, which is generally expensive, fixed in location, and unsuitable for continuous monitoring across multiple sites [18]. The MQ-7 and MQ-135 are low-cost MOS gas sensors with limited nominal detection ranges of approximately 20–2,000 ppm for CO and 10–1,000 ppm depending on the target gas, respectively. Direct exposure to concentrated vehicle exhaust may exceed these ranges and reduce quantitative reliability. Therefore, the proposed system is intended for preliminary emission screening, while controlled sample dilution is recommended for future improvement. Detailed specifications of the hardware components used in the system are summarized in Table 2. The IoT and alerting components provide supporting functionality for real-time visualization and notification, while the experimental focus of this study is the characterization, processing, and preliminary validation of low-cost gas-sensor responses under vehicle exhaust conditions.

Table 2. System component specifications

Component	Specification	Function
ESP32 Microcontroller	240 MHz dual-core, Wi-Fi & Bluetooth	Central processing; wireless data transmission
MQ-7 Gas Sensor	Range: 20–2,000 ppm CO; analog output	Carbon monoxide (CO) detection
MQ-135 Gas Sensor	Range: 10–1,000 ppm; detects CO_2, NH_3, NO_x	CO_2 and air quality monitoring
OLED Display (0.96")	128×64 px; I²C (SDA: pin 21, SCL: pin 22)	On-device real-time visualization
LED Indicators (×3)	Green / Yellow / Red; 1 kΩ carbon resistor each	Visual status: Level 1 / Level 2 / Level 3
Active Buzzer	I/O: pin 27; VCC: 3.3 V	Auditory hazard alarm
Blynk IoT Platform	Cloud-based dashboard; Wi-Fi (TCP/IP)	Real-time remote monitoring (smartphone & laptop)
Power Supply	2 × 18650 Li-ion batteries connected in series (7.4 V nominal, 8.4 V fully charged); LM2596 DC-DC step-down converter regulated to 5 V	Provides regulated power to the ESP32, gas sensors, display, and peripheral circuits

2.2. Hardware design

The monitoring device is installed within an acrylic enclosure measuring approximately 50 cm, providing protection for the electronic components while maintaining portability. At the core of the system is the ESP32 microcontroller, which functions as the main processing unit and offers dual-core processing capabilities operating at 240 MHz, along with built-in Wi-Fi connectivity for cloud-based communication [12], [18]. Gas detection is performed using two metal-oxide semiconductor sensors: the MQ-7 for CO detection and the MQ-135 for estimating CO_2-related gas responses. The MQ-135 is a non-selective sensor that is also sensitive to gases such as NH_3 and NO_x. Therefore, its output should not be interpreted as a selective CO_2 measurement. In the present prototype, no dedicated gas-separation, moisture-removal, or interference-compensation stage was implemented; consequently, the MQ-135-derived values are treated as approximate CO_2-related estimates [12], [16], [17]. Both MQ-series sensors are powered from the regulated 5-V supply rail rather than from the ESP32 GPIO pins. The analog output of the MQ-7 is connected to GPIO 33, while the analog output of the MQ-135 is connected to GPIO 32; therefore, these GPIO pins function only as ADC signal inputs. A common ground is maintained between the sensor supply and the ESP32 to provide a consistent reference for analog measurements. The revised electrical schematic clearly separates the MQ sensor power connections from their analog signal paths [13]. To provide immediate user feedback, the system incorporates three LED indicators green, yellow, and red each paired with a 1 kΩ current-limiting resistor to represent different emission levels. In addition, an active buzzer connected to GPIO 27 and powered by 3.3 V generates audible Level 2s when hazardous gas concentrations are detected. This combination of visual and audio indicators follows the design principles commonly adopted in recent IoT-based gas monitoring systems [14], [18]. The complete electrical schematic of the proposed system is presented in Figure 1, showing the ESP32 connections, sensor interfaces, power-supply rails, OLED communication lines, LED indicators, buzzer circuit, and grounding arrangement.

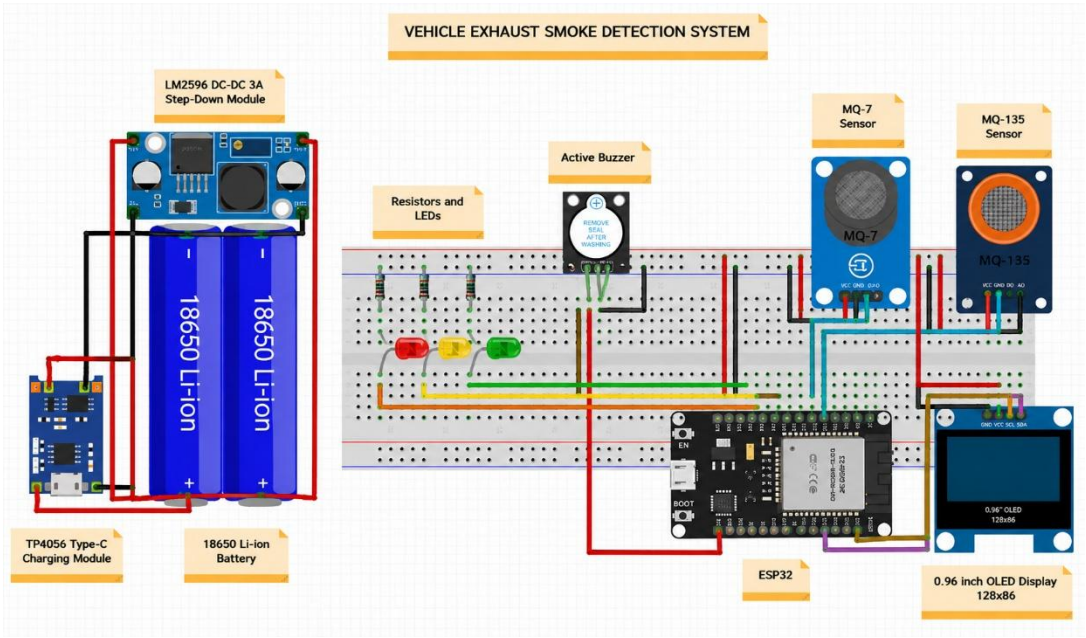


Figure 1. Electrical schematic of the proposed IoT-based vehicle exhaust emission monitoring system

2.3. Operating principle and emission response classification

When the system is powered using a 3–5 V DC supply, the MQ-7 and MQ-135 gas sensors require an initial warm-up period of approximately 30 minutes to stabilize their internal heating elements and ensure reliable measurements [19], [20]. After stabilization, exhaust gases emitted from a vehicle's tailpipe are detected by the sensors, which generate analog voltage signals corresponding to the concentration of the measured gases. The analog sensor signals are acquired by the ESP32 through its analog-to-digital converter and converted into estimated gas concentrations using the sensor-resistance and calibration relationships described in Section 2.6. The conversion is based on the ratio between the sensor resistance under gas exposure (R_s) and its baseline resistance (R_0). The resulting values represent sensor-derived concentration

estimates and should not be interpreted as certified measurement values, particularly outside the calibrated response range. The measured values are subsequently categorized according to the three-level threshold system presented in Table 3, consisting of Level 1, Level 2, and Level 3 conditions based on seven combined CO and CO_2 concentration scenarios. This hierarchical Level 2 mechanism, which has been successfully implemented in similar IoT-based emission monitoring applications [21], addresses a limitation commonly found in many low-cost monitoring platforms that lack graduated alert functionality [11], [12]. By providing multiple Level 2 levels, the system enables more effective early detection of hazardous emission conditions in practical field applications. The processed data are displayed locally on the OLED screen while being transmitted simultaneously to the Blynk IoT platform for remote monitoring and visualization [13]. Under Level 1 operating conditions, the green LED remains illuminated, whereas Level 2 and Level 3 levels activate the yellow and red LEDs, respectively, along with an audible buzzer alarm to notify users of elevated emission concentrations.

Table 3. Emission status threshold classification

CO (ppm)	CO (%)	CO_2 (ppm)	CO_2 (%)	Status
0 – 1,000	0 – 0.1	0 – 50,000	0 – 5	Level 1
0 – 1,000	0 – 0.1	60,000 – 150,000	6 – 15	Level 2
1,001 – 45,000	0.1 – 4.5	0 – 50,000	0 – 5	Level 2
1,001 – 45,000	0.1 – 4.5	60,000 – 150,000	6 – 15	Level 2
0 – 1,000	0 – 0.1	> 160,000	> 16	Level 3
1,001 – 45,000	0.1 – 4.5	> 160,000	> 16	Level 3
> 45,000	> 4.5	> 160,000	> 16	Level 3

2.4. Software implementation

The system firmware was developed using the Arduino IDE with C/C++ programming language and uploaded to the ESP32 microcontroller through a USB connection, following the software development approach commonly adopted in MQ-sensor-based IoT monitoring applications [12], [18], [21]. The software is responsible for several key functions, including the acquisition of analog sensor data and its conversion into gas concentration values expressed in parts per million (ppm) using calibration equations derived from sensor characteristics. In addition, the program performs threshold evaluation based on the status categories defined in Table 2, allowing the system to classify emission levels into predefined conditions. The firmware also manages real-time updates on the OLED display, presenting current CO and CO_2 concentrations along with their corresponding status indicators. Furthermore, the ESP32 utilizes its integrated Wi-Fi capability to establish communication with the Blynk IoT cloud platform, enabling continuous data synchronization and remote access [13]. The Blynk dashboard was designed with interactive gauges and time-series graphs to visualize emission data in real time through both the mobile application and web-based interface. This configuration allows users to monitor measurements simultaneously through the local display and remote cloud platform, providing a dual-monitoring capability that remains limited or absent in many previously reported IoT-based emission monitoring systems [11]–[17].

2.5. Experimental setup and test vehicle

Emission testing was performed on ten vehicles manufactured between 1978 and 2023, consisting of five motorcycles and five passenger cars. The ten vehicles were selected to provide an exploratory comparison across different manufacturing years and engine technologies. Because the sample size is limited, the experiment is intended as a preliminary system-performance evaluation rather than a statistically representative assessment of the broader vehicle population. The broad manufacturing range was intentionally selected to facilitate a comparative analysis of exhaust emissions produced by older and newer engine technologies, an aspect that remains insufficiently explored in previous IoT-based vehicle emission monitoring studies [11], [18]–[20]. The measured emission characteristics were evaluated according to the vehicle emission regulations established by the Indonesian Ministry of Environment and Forestry (MoEF), which have gradually implemented emission standards equivalent to the Euro regulations, beginning with Euro 2 in 2003 and advancing to Euro 4 for gasoline-powered vehicles in 2018 and diesel-powered vehicles in 2022 [22]–[25]. Based on these regulations, motorcycles manufactured before 2010 are required to comply with maximum limits of 5.5% CO and 2,200 ppm HC, while motorcycles produced between 2010 and 2016 must satisfy stricter limits of 4% CO and 1,800 ppm HC. Vehicles manufactured after 2016 are subject to even more rigorous emission requirements. In this study, vehicle age and engine technology were considered independent variables influencing exhaust emission performance, following methodologies commonly employed in vehicle emission characterization research [6], [9], [24]–[27]. Detailed specifications of all tested vehicles are presented in Table 4.

Table 4. Test vehicle specifications

No.	Vehicle	Engine Type	Displacement	Year
M1	Vespa 90 CC	2-stroke	90 CC	1978
M2	Honda GL100	4-stroke	160 CC	1996
M3	Honda Win 100	4-stroke	100 CC	2004
M4	Yamaha SoulGT	4-stroke	113 CC	2012
M5	Yamaha Fazio	4-stroke	125 CC	2022
C1	Toyota Starlet	Gasoline	1,000 CC	1996
C2	Suzuki APV	Gasoline	1,500 CC	2008
C3	Toyota Rush	Gasoline	1,500 CC	2016
C4	Mitsubishi Pajero Sport Dakar	Diesel	2,442 CC	2017
C5	Daihatsu Xenia	Gasoline	1,496 CC	2023

For each vehicle, the gas sensor probe was positioned at the exhaust tailpipe for at least three minutes after sensor warm-up and stabilization, following standard idle-condition emission testing procedures [28], [29]. Measurements were primarily conducted at idle speed, with additional higher-engine-speed tests performed when required. Sensor readings were displayed in real time on the OLED and transmitted to the Blynk dashboard for remote monitoring and data recording [30]. To evaluate system accuracy, selected vehicles were also tested using a standard automotive exhaust gas analyzer, and the results were compared with the proposed device to identify measurement errors and sensor limitations [31].

2.6. Sensor calibration

Before conducting emission measurements, the MQ-7 and MQ-135 sensors were preheated for approximately 30 minutes in clean ambient air to stabilize their baseline responses. The baseline resistance (R_0) was established during the calibration procedure, while the sensor resistance under gas exposure (R_s) was calculated from the measured analog response. The ratio (R_s/R_0) was subsequently used as the primary input for the sensor-response conversion model. The calibration relationship was applied to convert the measured sensor response into an estimated gas concentration [12], [14], [21]. However, the resulting concentration values are quantitatively meaningful only within the response interval for which the sensor calibration is considered valid. When direct exhaust exposure produces sensor responses corresponding to concentrations beyond the nominal operating range of the MQ-7 or MQ-135, the conversion equation effectively involves extrapolation beyond the sensor's recommended quantitative range. Such extrapolated values are therefore interpreted as indicative high-concentration estimates and are not considered traceable reference measurements.

The sensor resistance Rs was calculated from the measured sensor-output voltage using the voltage-divider relationship:

$$R_s = R_L \left(\frac{V_c}{V_{out}} - 1 \right) \tag{1}$$

where R_L is the load resistance V_c is the sensor supply voltage, and V_{out} is the measured analog-output voltage. The baseline resistance R_0 was determined during calibration in clear air as:

$$R_0 = \frac{R_{s,clean}}{\frac{R_s}{R_0}} \tag{2}$$

where $R_{s,clean}$ represents the sensor resistance measured after the warm-up period. The normalized sensor response was then calculated as:

$$r = \frac{R_s}{R_0} \tag{3}$$

Gas concentration was estimated using a power-law relationship derived from the sensor response characteristic:

$$C = a \left(\frac{R_s}{R_0} \right)^b \tag{4}$$

where C is the estimated gas concentration in ppm, while a dan b are celibration coeficients determined for the target gas.

No controlled gas-dilution stage was incorporated into the current prototype. Consequently, the direct tailpipe measurements reported in this study should be interpreted with particular caution when the estimated concentration exceeds the nominal sensor range. The comparison with the standardized automotive exhaust gas analyzer was consequently used to examine the level of agreement observed at selected experimental points rather than to establish metrological accuracy across the complete exhaust concentration range. Future calibration will incorporate controlled sample dilution and multi-point calibration using certified reference gases so that the exhaust samples can be maintained within the validated response ranges of the sensors. This approach is expected to reduce extrapolation error and improve the quantitative reliability of subsequent measurements [18], [24], [32].

3. RESULTS AND DISCUSSION

3.1. System implementation

The developed IoT-based vehicle exhaust emission monitoring device is constructed using two separate acrylic enclosures mounted on a 50 cm support structure. The first enclosure accommodates the main electronic components, including the ESP32 microcontroller, LED indicators, resistors, buzzer, lithium-ion battery, LM2596 3A DC-DC step-down converter, TP4056 USB Type-C charging module, and the printed circuit board (PCB). Meanwhile, the second enclosure contains the MQ-7 and MQ-135 gas sensors, which are strategically positioned to allow direct exposure to vehicle exhaust gases at the tailpipe outlet. This dual-enclosure configuration is intended to separate the gas-sensing components from heat-producing electronic circuits, thereby minimizing thermal effects that could influence sensor performance and measurement accuracy. Before each testing session, the sensors were calibrated according to the emission threshold criteria presented in Table 2, and measurement stability was verified following a warm-up period of approximately 30 minutes, in accordance with the manufacturer's recommended preheating procedure. The successful implementation and physical realization of the proposed monitoring system are illustrated in Figure 2.



Figure 2. Physical implementation of the developed prototype

3.2. Motorcycle emission measurement result

Table 5 presents the results of CO and CO_2 emission measurements obtained from five motorcycles manufactured between 1978 and 2022. Based on the threshold classification implemented in the proposed monitoring system, all tested motorcycles were categorized as being in the Level 2 condition. This classification indicates that the measured carbon monoxide (CO) concentrations were within the range of 1,001–45,000 ppm, while carbon dioxide (CO_2) concentrations were recorded between 60,000 and 150,000 ppm, according to the criteria established in Table 2. The findings suggest that, although the emission levels did not reach the Level 3 category, all motorcycles produced exhaust gas concentrations exceeding the Level 1 threshold, thereby requiring attention and indicating the presence of moderate emission levels during testing.

Table 5. Motorcycle emission measurement result

No.	Vehicle	Year	CC	CO (ppm)	CO (%)	CO_2 (ppm)	CO_2 (%)	Status
1	Vespa 90 CC	1978	90	2,074	0.20	93,600	9.3	Level 2
2	Honda GL100	1996	160	3,440	0.34	121,440	12.1	Level 2
3	Honda Win 100	2004	100	4,043	0.40	122,850	12.2	Level 2
4	Yamaha SoulGT	2012	113	2,755	0.27	122,850	12.2	Level 2
5	Yamaha Fazio	2022	125	1,983	0.19	98,700	9.8	Level 2

The analysis of motorcycle emission data indicates a noticeable correlation between vehicle age and the level of exhaust pollutants produced. Among the tested motorcycles, the Honda Win 100 (2004, 100 CC) exhibited the highest emission levels, recording a CO concentration of 4,043 ppm (0.40%) and a CO_2 concentration of 122,850 ppm (12.2%). In contrast, the Yamaha Fazio (2022, 125 CC), representing a newer generation of motorcycle technology, produced the lowest emissions, with CO and CO_2 concentrations of 1,983 ppm (0.19%) and 98,700 ppm (9.8%), respectively. The results further suggest that engine displacement is not the primary factor influencing emission magnitude. For example, the Honda Win 100, despite having a smaller engine capacity of 100 CC, generated higher CO emissions than the Honda GL100 (160 CC), which recorded 3,440 ppm. This finding supports previous studies indicating that vehicle age, engine condition, and combustion technology have a greater impact on exhaust emissions than engine size alone [6], [9]. Furthermore, the Vespa two-stroke motorcycle manufactured in 1978 (90 CC) produced CO and CO_2 concentrations of 2,074 ppm (0.20%) and 93,600 ppm (9.3%), respectively. Although its engine displacement was relatively small, the observed emission levels reflect the lower combustion efficiency typically associated with two-stroke engine designs [9], [18]. Overall, these results align with existing literature demonstrating that aging engines and declining catalytic converter effectiveness contribute significantly to increased CO emissions in older vehicles.

3.3. Car emission measurement result

Table 6 presents the emission measurement results for five automobiles ranging from 1996 to 2023. All tested vehicles were similarly classified under the Level 2 status for CO_2, while CO concentrations for newer vehicles approached the lower boundary of the Level 2 threshold.

Table 6. Automobile emission measurement result

No.	Vehicle	Year	CC	CO (ppm)	CO (%)	CO_2 (ppm)	CO_2 (%)	Status
1	Toyota Starlet	1996	1,000	2,353	0.23	89,970	8.9	Level 2
2	Suzuki APV	2008	1,500	3,863	0.38	120,630	12.0	Level 2
3	Toyota Rush	2016	1,500	1,723	0.17	80,370	8.0	Level 2
4	Mitsubishi Pajero Sport	2017	2,442	1,200	0.12	46,050	4.6	Level 2
5	Daihatsu Xenia	2023	1,496	1,776	0.17	84,810	8.4	Level 2

Among the automobiles tested, the Suzuki APV (2008, 1,500 CC) produced the highest emission levels, recording a CO concentration of 3,863 ppm (0.38%) and a CO_2 concentration of 120,630 ppm (12.0%). In contrast, the Mitsubishi Pajero Sport Dakar (2017, 2,442 CC) exhibited the lowest emissions, with CO measured at 1,200 ppm (0.12%) and CO_2 at 46,050 ppm (4.6%), despite having the largest engine displacement among all tested vehicles. These findings indicate that engine displacement alone does not directly determine emission levels. Instead, factors such as engine technology, combustion efficiency, and vehicle maintenance play a more significant role in influencing exhaust gas emissions. This trend becomes particularly evident when comparing the Suzuki APV 2008 (1,500 CC) with the Daihatsu Xenia 2023 (1,496 CC), two vehicles with nearly identical engine capacities. The newer Daihatsu Xenia demonstrated approximately 54% lower CO emissions and 30% lower CO_2 emissions, highlighting the impact of advancements in fuel injection systems, combustion management, and catalytic converter technology. A similar pattern was observed in the comparison between the Toyota Starlet 1996 (1,000 CC) and the Toyota Rush 2016 (1,500 CC). Although the Starlet has a smaller engine, it generated higher emission levels, recording 2,353 ppm (0.23%) CO and 89,970 ppm (8.9%) CO_2, compared to the Toyota Rush, which produced 1,723 ppm (0.17%) CO and 80,370 ppm (8.0%) CO_2. These results further support the overall findings of this study, demonstrating that vehicle age and technological advancements have a greater influence on emission performance than engine displacement across both motorcycle and automobile categories.

3.4. System validation against standardized reference instruments

To evaluate the measurement agreement between the developed system and a standardized automotive exhaust gas analyzer, emission readings from six selected vehicles were compared with those obtained from the reference instrument, emission readings from the developed system were compared against data from a certified standardized automotive exhaust gas analyzer for a subset of six vehicles (three automobiles and three motorcycles). Comparison results are presented in Tables 7 and 8, where ΔCO and ΔCO_2 denote the absolute differences between the developed system and the reference instrument.

Table 7. Validation comparison automobile emission measurements

No.	Vehicle	Year	CO Dev. (%)	CO Ref. (%)	CO_2 Dev. (%)	CO_2 Ref. (%)	ΔCO (%)	ΔCO_2 (%)
1	Suzuki APV	2008	0.39	0.40	12.1	12.6	0.01	0.5
2	Toyota Rush	2016	0.17	0.30	8.0	8.4	0.13	0.4
3	Daihatsu Xenia	2023	0.18	0.20	8.5	8.9	0.02	0.4

Table 8. Validation comparison motorcycle emission measurements

No.	Vehicle	Year	CO Dev. (%)	CO Ref. (%)	CO_2 Dev. (%)	CO_2 Ref. (%)	ΔCO (%)	ΔCO_2 (%)
1	Vespa 90 CC	1978	0.21	0.31	9.4	9.6	0.10	0.2
2	Yamaha SoulGT	2012	0.28	0.30	12.3	12.7	0.02	0.4
3	Yamaha Fazio	2022	0.20	0.21	9.9	9.8	0.01	0.1

For automobile measurements (Table 6), the developed system demonstrated close agreement with the reference instrument. The smallest deviation was recorded for the Suzuki APV 2008, with ΔCO = 0.01% and ΔCO_2 = 0.5%. The largest CO deviation occurred for the Toyota Rush 2016 (ΔCO = 0.13%), likely attributable to the lower absolute CO concentration at that vehicle's operating condition, which increases relative measurement sensitivity. CO_2 deviations were relatively small at the selected test points. However, because the MQ-135 is inherently cross-sensitive to other exhaust constituents, these differences should be interpreted only as pointwise agreement with the reference analyzer under the specific experimental conditions and not as evidence of selective or high-accuracy CO_2 measurement.

The validation results for motorcycle emission measurements presented in Table 7 indicate that the Yamaha Fazio 2022 achieved the highest level of agreement with the reference exhaust gas analyzer. This vehicle recorded the smallest measurement deviations, with ΔCO = 0.01% and ΔCO_2 = 0.1%, representing the best overall performance among the six validated vehicles. In contrast, the Vespa 1978 exhibited the largest discrepancy in CO measurements, with a ΔCO value of 0.10%. This greater deviation may be attributed to the less stable combustion characteristics and higher emission levels typically associated with older vehicle technologies, which can increase measurement variability when using low-cost gas sensors. The Yamaha SoulGT 2012 demonstrated moderate performance, producing deviations of ΔCO = 0.02% and ΔCO_2 = 0.4%, indicating a relatively good level of measurement accuracy. In general, the proposed monitoring system tended to slightly underestimate CO concentrations when compared with the standardized reference instrument, particularly for older vehicles with higher emission outputs. Conversely, measurements obtained from newer vehicles showed closer agreement with the reference analyzer, reflecting improved sensor performance under more stable combustion conditions. These findings are consistent with previous studies involving IoT-based vehicle emission monitoring systems, which have reported similar trends in sensor accuracy and measurement reliability. Therefore, the developed system can be considered a practical solution for preliminary vehicle emission screening and environmental monitoring applications, especially for modern vehicles. Nevertheless, additional calibration optimization and sensor characterization are recommended to further enhance measurement accuracy and reduce deviations when testing older, high-emission vehicles. The prototype did not incorporate selective gas separation, humidity compensation, or compensation for interfering gases such as NH_3 and NO_x. Therefore, the MQ-135-derived values should be regarded as approximate CO_2-related estimates, and the observed agreement should not be generalized as evidence of high-accuracy CO_2 sensing.

3.5. Comparative analysis: vehicle exhaust vs. waste combustion smoke

To contextualize vehicle emission levels, an additional test was conducted comparing the CO and CO_2 output of vehicle exhaust against waste combustion smoke under ambient conditions. Results are presented in Table 9.

The comparison results show a substantial difference between emissions generated from waste combustion and those produced by vehicle exhaust. Smoke from waste burning recorded a CO concentration of 140 ppm (0.01%) and a CO_2 concentration of 4,920 ppm (0.49%), placing it within the Level 1 category

based on the threshold criteria established in Table 2. Conversely, vehicle exhaust emissions measured significantly higher values, with CO reaching 4,095 ppm (0.40%) and CO_2 reaching 115,200 ppm (11.5%), resulting in a Level 2 classification. Relative to waste combustion, vehicle exhaust generated approximately 29 times higher CO concentrations and 23 times higher CO_2 concentrations. These findings indicate that motor vehicles represent a considerably more concentrated source of combustion-related pollutants at the measurement location compared to open waste burning. The observed results support previous studies identifying transportation emissions as a major contributor to elevated CO and CO_2 levels in urban environments, particularly in densely populated Indonesian cities. Furthermore, the developed monitoring system successfully differentiated between the two emission sources and correctly assigned their respective classifications according to the predefined threshold levels, demonstrating its effectiveness in distinguishing emission profiles with substantially different pollutant concentrations and environmental impacts

Table 9. Comparative emission levels: vehicle exhaust vs. waste combustion smoke

No.	Sample	CO (ppm)	CO (%)	CO_2 (ppm)	CO_2 (%)	Status
1	Waste combustion smoke	140	0.01	4,920	0.49	Level 1
2	Vehicle exhaust	4,095	0.40	115,200	11.5	Level 2

3.6. Overall system performance assessment

The experimental evaluation showed that the proposed IoT-based vehicle emission monitoring system operated effectively and consistently. The MQ-7 and MQ-135 sensors successfully measured CO and CO_2 concentrations from all ten tested vehicles, while data were continuously transmitted to the OLED display, Blynk mobile application, and web dashboard without communication failures. The LED and buzzer alerts also responded correctly when sensor readings exceeded the programmed prototype thresholds, confirming the effectiveness of the threshold-based control logic. The system further provides dual monitoring through local and cloud-based interfaces. However, the MQ-series sensors required recovery time after exposure to high exhaust concentrations, which may delay subsequent measurements. Future improvements may include active air purging, enhanced calibration, and multi-sensor arrays to improve recovery and real-time monitoring performance.

4. CONCLUSION

This study developed and experimentally evaluated a portable IoT-based vehicle exhaust monitoring prototype integrating an ESP32 microcontroller, MQ-7 and MQ-135 gas sensors, an OLED display, LED and buzzer indicators, and the Blynk IoT platform. The system successfully acquired sensor responses from the tested vehicles and transmitted measurement information to both local and remote monitoring interfaces. The experimental results demonstrated variations in sensor response among vehicles of different manufacturing years and engine technologies. However, several of the estimated exhaust-gas concentrations exceeded the nominal quantitative operating ranges of the MQ-series sensors. Because the present prototype employed direct tailpipe sampling without a controlled dilution stage, concentration values obtained beyond the calibrated sensor range should be interpreted as indicative or semi-quantitative estimates rather than precise reference measurements.

Comparison with a standardized automotive exhaust gas analyzer showed varying levels of agreement at the selected experimental points. The reported differences represent absolute differences between the prototype and reference measurements under the specific test conditions and should not be interpreted as a complete measurement-accuracy specification. Therefore, the proposed system is more appropriately considered a preliminary low-cost emission-screening and monitoring platform rather than a substitute for certified regulatory emission-measurement equipment. Future development should incorporate a controlled exhaust-sample dilution and conditioning system to maintain gas concentrations within the validated operating ranges of the sensors. Multi-point calibration using certified reference gases, repeated measurements, environmental compensation, and formal uncertainty analysis should also be implemented to improve quantitative reliability. Additional improvements, including better separation of the sensing and processing electronics, database integration, web-based monitoring, and GPS-based geolocation, may further support the application of the system in long-term vehicle-emission monitoring and intelligent transportation environments.

ACKNOWLEDGMENTS

The authors acknowledge the use of ChatGPT (OpenAI, GPT-5.5) for language refinement and figure editing during the preparation of this manuscript. All suggestions and modifications generated with AI assistance were reviewed and validated by the authors, who assume full responsibility for the content and conclusions presented in this work.

FUNDING INFORMATION

The authors gratefully acknowledge the financial support provided by the Non-Tax State Revenue Fund (BLU) of State Polytechnic of Ujung Pandang, which made this research possible. The authors also wish to thank the Department of Electrical Engineering and all laboratory staff at Politeknik Negeri Ujung Pandang for providing access to equipment and technical facilities throughout the course of this study.

AUTHOR CONTRIBUTIONS STATEMENT

This journal uses the Contributor Roles Taxonomy (CRediT) to recognize individual author contributions, reduce authorship disputes, and facilitate collaboration.

Name of Author	C	M	So	Va	Fo	I	R	D	O	E	Vi	Su	P	Fu
Nuraeni Umar	✓	✓	✓	✓	✓	✓		✓	✓	✓			✓	✓
Riesa Krisna Astuti Sakir		✓				✓		✓	✓	✓	✓	✓		
Muhira Dzar Faraby	✓		✓	✓			✓			✓	✓		✓	✓
Sufianti Munirman				✓		✓			✓					
Asma Amaliah	✓		✓		✓		✓		✓	✓		✓		✓
Andi Mutiah Nurul Aini	✓		✓			✓				✓				
Latifah Wulandari	✓		✓			✓				✓				
Nurhayati	✓		✓			✓				✓				
Yuli Asmi Rahman				✓	✓			✓		✓	✓		✓	✓
Andi Nur Putri		✓		✓			✓			✓	✓		✓	✓

C : **C**onceptualization
M : **M**ethodology
So : **So**ftware
Va : **Va**lidation
Fo : **Fo**rmal analysis
I : **I**nvestigation
R : **R**esources
D : **D**ata Curation
O : Writing - **O**riginal Draft
E : Writing - Review & **E**diting
Vi : **Vi**sualization
Su : **Su**pervision
P : **P**roject administration
Fu : **Fu**nding acquisition

CONFLICT OF INTEREST STATEMENT

Authors state no conflict of interest.

DATA AVAILABILITY

The data that support the findings of this study are available from the corresponding author, [initials: NU], upon reasonable request.

REFERENCES

[1] World Health Organization (WHO), "WHO ambient air quality database (Update Jan 2024)," 2024. https://www.who.int/publications/m/item/who-ambient-air-quality-database-(update-jan-2024) (accessed Oct. 01, 2026).
[2] Health Effects Institute, "State of Global Air 2025: A report on air pollution and its role in the world's leading causes of death," 2025. https://www.stateofglobalair.org/resources/report/state-global-air-report-2025 (accessed Oct. 01, 2026).
[3] Institute for Health Metrics and Evaluation (IHME), "New report shows nearly 9 of 10 global air pollution deaths are from noncommunicable diseases," 2025. https://www.healthdata.org/news-events/newsroom (accessed Oct. 01, 2026).
[4] Institute for Essential Services Reform (IESR), "Emission reduction in transportation," 2023. https://iesr.or.id/en/emission-reduction-in-transportation/ (accessed Oct. 01, 2026).
[5] Institute for Essential Services Reform (IESR), "National and regional low-emission transportation policy roadmap," 2023. https://iesr.or.id/en/national-and-regional-low-emission-transportation-policy-roadmap/ (accessed Oct. 01, 2026).
[6] F. M. Felayati, U. Prayogi, B. Ariani, and N. S. Octaviani, "Experimental study of dual-fuel diesel/CNG engine performance and emissions with oxy-hydrogen injection by variable location," *International Journal on Engineering Applications (IREA)*, vol. 13, no. 4, p. 412, Jul. 2025, doi: 10.15866/irea.v13i4.25625.

[7] Climate Impact Tracker, "Tracking air pollution in Indonesia and the policies changing it," 2025. https://www.climateimpacttracker.com/air-pollution-indonesia/ (accessed Oct. 01, 2026).
[8] T. Abdallah, "Sustainable elements of bus networks," in *Sustainable Mass Transit*, Elsevier, 2023, pp. 111–125. doi: 10.1016/B978-0-443-15271-9.00014-5.
[9] V. Thana Singam, H. Mohd Zahari, and N. Mohamad Rafiuddin, "A systematic review on carbon emission of light duty vehicles in urban environment," *Social Sciences & Humanities Open*, vol. 10, p. 100924, 2024, doi: 10.1016/j.ssaho.2024.100924.
[10] California Air Resources Board (CARB), "Car & bus exposure studies: Health effects from vehicle pollution," 2024. https://ww2.arb.ca.gov/resources/documents/car-bus-exposure-studies (accessed Oct. 01, 2026).
[11] T. L. Narayana *et al.*, "Advances in real time smart monitoring of environmental parameters using IoT and sensors," *Heliyon*, vol. 10, no. 7, p. e28195, Apr. 2024, doi: 10.1016/j.heliyon.2024.e28195.
[12] L. M. Easterline, A. A.-Z. R. Putri, P. S. Atmaja, A. L. Dewi, and A. Prasetyo, "Smart air monitoring with IoT-based MQ-2, MQ-7, MQ-8, and MQ-135 sensors using NodeMCU ESP32," *Procedia Computer Science*, vol. 245, pp. 815–824, 2024, doi: 10.1016/j.procs.2024.10.308.
[13] A. Das, B. M. Chandrakala, N. Shobha, J. Reshma, V. Bhoothpur, and R. Kumar Godi, "IoT based air quality monitoring and asthma alerts driven by non-crossing quantile regression neural networks," *Biomedical Signal Processing and Control*, vol. 119, p. 109565, Jun. 2026, doi: 10.1016/j.bspc.2026.109565.
[14] N. Nurhayati, M. D. Faraby, A. Asriyadi, M. L. Mustam, and M. Mukhlisin, "Implementation of Internet of Things (IoT) for automated flower plant irrigation system," *International Review on Modelling and Simulations (IREMOS)*, vol. 18, no. 4, p. 279, Aug. 2025, doi: 10.15866/iremos.v18i4.26851.
[15] M. A. Saktiono, S. Soemarno, G. Ciptadi, and S. Wahyudi, "Development of air quality monitoring device (AQM Dev) for air quality measurement," *International Journal on Engineering Applications (IREA)*, vol. 12, no. 2, p. 119, Mar. 2024, doi: 10.15866/irea.v12i2.24449.
[16] M. A. Saktiono, S. Soemarno, G. Ciptadi, and S. Wahyudi, "Air quality prediction model of Surabaya City using long short term memory (LSTM) method," *International Journal on Engineering Applications (IREA)*, vol. 12, no. 1, p. 69, Jan. 2024, doi: 10.15866/irea.v12i1.24289.
[17] Y. V. Vivek, K. Umamaheswari, T. Sriharika, and R. Nikesh, "IOT-based ESP32-driven real-time air quality monitoring and purification," *Grenze International Journal of Engineering \& Technology (GIJET)*, vol. 11, no. Part2, p. 1248, 2025.
[18] O. Farrag, A. Mansour, B. Abed, A. Abu Alhaj, T. Landolsi, and A. R. Al-Ali, "IVEMPS: IoT-based vehicle emission monitoring and prediction system," *IEEE Access*, vol. 13, pp. 95628–95646, 2025, doi: 10.1109/ACCESS.2025.3572726.
[19] J. C. Priya, D. Balasubramanian, R. N. S. Shen, C. W. Onn, U. Kale, and J. Matijošius, "A decentralized blockchain-based smart framework for continuous vehicle emission monitoring in smart cities," *Scientific Reports*, vol. 15, no. 1, p. 39343, Nov. 2025, doi: 10.1038/s41598-025-22925-z.
[20] S. Kamal Sundar, R. Kaushik, A. Shukla, R. Srinikesh, and P. Jayanthi, "A predictive IoT framework for continuous vehicle emission monitoring using ensemble CatBoost and XGBoost Learning," in *2026 International Conference on Data Science, Agents and Artificial Intelligence (ICDSAAI)*, Mar. 2026, pp. 1–5. doi: 10.1109/ICDSAAI69492.2026.11505117.
[21] D. H. Hareva, J. Adhitthana, I. M. Murwantara, K. Prasetya, and Hery, "A cloud-based system for visualizing indoor air quality using AQI Guidelines," *Procedia Computer Science*, vol. 269, pp. 278–288, 2025, doi: 10.1016/j.procs.2025.08.280.
[22] F. H. Rimu, D. Q. Rich, G. M. Lemley, and P. K. Hopke, "Trends in New York State light-duty vehicle fleet composition: Emission standards and engine technology (2013–2025)," *Atmospheric Pollution Research*, vol. 17, no. 5, p. 102904, May 2026, doi: 10.1016/j.apr.2026.102904.
[23] T. Nawal, O.-A. Omar, M. Smail, and B. Aissa, "Optimized fractional-order direct torque control with space vector modulation strategy for two-wheel-drive electric vehicles," *International Journal of Electrical and Computer Engineering (IJECE)*, vol. 15, no. 5, p. 4409, Oct. 2025, doi: 10.11591/ijece.v15i5.pp4409-4420.
[24] K. Lee, Y. Bernard, T. Dallmann, U. Tietge, I. Pniewska, and I. Rintanen, "Measurement of real-world motor vehicle emissions in Jakarta," 2024. https://trueinitiative.org/wp-content/uploads/2024/11/true-jakarta-report-en.pdf (accessed Oct. 01, 2026).
[25] A. G. Osman, M. Tawfik, A. M. Ali, and M. S. Asfoor, "Evaluation of electric vehicle performance based on high-fidelity modeling and experimental testing," in *2024 6th Novel Intelligent and Leading Emerging Sciences Conference (NILES)*, Oct. 2024, pp. 50–55. doi: 10.1109/NILES63360.2024.10753161.
[26] L. Yang *et al.*, "Evaluating the effectiveness of tightened emission standards in reducing real-world vehicle emissions: Evidence from on-road testing and inventory analysis," *Journal of Cleaner Production*, vol. 559, p. 148288, May 2026, doi: 10.1016/j.jclepro.2026.148288.
[27] S.-H. Woo, W. Kim, M. Kim, H. Jang, and S. Lee, "Impact of vehicle electrification on brake wear particle (BWP) emissions under real-world driving conditions," *Wear*, vol. 584–585, p. 206392, Jan. 2026, doi: 10.1016/j.wear.2025.206392.
[28] A. Wang, M. Wang, Z. Yuan, X. Liu, and Q. Sha, "Vehicular VOC speciation dynamics under China's progressive emission standards: Mechanistic drivers from real-time monitoring," *Journal of Cleaner Production*, vol. 538, p. 147350, Jan. 2026, doi: 10.1016/j.jclepro.2025.147350.
[29] M. J. Kyando, J. W. Ntalikwa, and T. Kivevele, "Compressed natural gas in aged internal combustion engines: performance, emissions, and challenges – a systematic review," *Energy Conversion and Management: X*, vol. 30, p. 101726, May 2026, doi: 10.1016/j.ecmx.2026.101726.
[30] B. Méndez and P. Lamo, "IoT node for monitoring and traceability of live plants in maritime transport," *Array*, vol. 29, p. 100621, Mar. 2026, doi: 10.1016/j.array.2025.100621.
[31] H. A. H. Al-Hamzawi, A. S. A. Al Sailawi, R. Z. Homod, H. A. yemma Kadhim, H. I. Mohammed, and M. A. Al-Shareeda, "Machine learning-enhanced optimization of exhaust gas recirculation strategies for superior diesel engine performance and emissions control: A synergistic experimental and computational study," *International Journal of Hydrogen Energy*, vol. 169, p. 151184, Sep. 2025, doi: 10.1016/j.ijhydene.2025.151184.
[32] A. Mohan, M. P.V, and U. Subramaniam, "A comprehensive review on the integration of air quality monitoring systems with hybrid electric vehicles for emission control in smart cities," *Science of The Total Environment*, vol. 994, p. 180022, Sep. 2025, doi: 10.1016/j.scitotenv.2025.180022.

BIOGRAPHIES OF AUTHORS



Nuraeni Umar received her bachelor's degree in electrical engineering from Hasanuddin University, Indonesia, in 1996, a Master of Technology in Electrical Engineering specializing system Telecommunication Engineering from Institut Teknologi Bandung, Indonesia, in 2005. She is a lecturer in Electrical Engineering Department, Telecommunication Faculty, Ujung Pandang State Polytechnic, Makassar, Indonesia, from 1987. Her research interests include telecommunication system. She can be contacted at nuraeni_umar@poliupg.ac.id.



Riesa Krisna Astuti Sakir received her bachelor's degree in Electrical Engineering from Telkom University, Indonesia in 2017 and master's degree in IT Convergence Engineering from Kumoh National Institute of Technology, South Korea, in 2020. She is currently a junior lecturer in Telecommunication study program, Department of Electrical Engineering, Ujung Pandang State Polytechnic, Makassar, Indonesia by 2022. Her research interests include wireless communication networks and Data Communication. She can be contacted at riesakrisna@poliupg.ac.id.



Muhira Dzar Faraby finished the S.T. and M.T. degree in 2012 and 2014 from Dept. of Electrical Engineering UNHAS, Indonesia and the Dr degree in 2021 from Dept. of Electrical Engineering, ITS Surabaya, Indonesia. Currently he's a lecturer in Dept of Electrical Engineering, PNUP, Indonesia. His researchs are PQ, Optimization of Power System, and Stability of Power Systems. He can be contacted at muhiradzarfaraby@poliupg.ac.id.



Sufianti Munirman was born in Ujung Pandang on March 11, 1997, She is a lecturer at the Ujung Pandang State Polytechnic, precisely in the Telecommunication Network Engineering Technology Study Program. She was started her undergraduate education (S1) in Electrical Engineering at the Indonesian Christian University Paulus Makassar and continued with her master's degree (S2) in Electrical Engineering at Hasanuddin University. She can be contacted at sufiantimunirman@poliupg.ac.id.



Asma Amaliah reveiced Bachelor degree (S.T.) in 2012 from Department of Electrical Engineering, Hasanuddin University, Indonesia. Master degree (M.T.) in 2016 from Department of Electrical Engineering, Hasanuddin University. Currently, she is a lecturer in Department of Electrical Engineering, Ujung Pandang State of Polytechnic, Indonesia. Her research interest in Digital Signal Processing and Embedded System. She can be contacted at asmaamaliah@poliupg.ac.id



Andi Mutiah Nurul Aini received her Associate Degree in Telecommunication Engineering, Department of Electrical Engineering from Ujung Pandang State Polytechnic in 2025. She can be contacted at her can be contacted at amnelee16@gmail.com.



Latifah Wulandari received her associate degree in Telecommunication Engineering, Department of Electrical Engineering from Ujung Pandang State Polytechnic in 2025. She can be contacted at her can be contacted by email: She can be contacted at latifahwulandari03@gmail.com.



Nurhayati received S.Si degree in 1997 from department of physics, University of Hasanuddin, Makassar, Indonesia. The M.T degree in 2005 from department of Electrical Engineering, Bandung Institute of Technology, Bandung, Indonesia. The Doctoral degree in 2022 from department of Engineering Vocation University State of Makassar, Indonesia. Currently she is a lecturer in Departement of Multimedia And Networking Engineering, Polytechnic State Ujung Pandang Makassar, Indonesia. Her research interest in embedded systems and the internet of things, in the vocational field of engineering. She can be contacted at Nurhayati_tmj@poliupg.ac.id



Yuli Asmi Rahman completed her S.T. degrees in 2003 from Dept. of Electrical Engineering at UNHAS, Indonesia. She completed M.T. degrees in 2010 form Dept, of Electrical Engineering at UGM, Indonesia. She completed Dr. Degree in 2020 from Dept. of Electrical Engineering UNHAS, Indonesia. Presently, she is a lecturer in Dept. of Electrical Engineering, Tadulako University, Indonesia. Her research focuses on Optimization of Renewable Energy, Power System Protection and Power Electronic Converters. She can be contacted at yuli.asmi@untad.ac.id



Andi Nur Putri received her bachelor's degree (S.Pd.) in Electrical Engineering from Universitas Negeri Makassar, Indonesia, in 2007. She obtained her master's degree (M.T) in Electrical Engineering from Universitas Hasanuddin, Makassar, Indonesia, in 2011. She completed her Doctoral degree (Dr.) in Electrical Engineering at Institut Teknologi Sepuluh Nopember (ITS), Surabaya, Indonesia, in 2025. She is currently a lecturer in the Department of Electrical Engineering at Universitas Patria Artha, Makassar, Indonesia. Her research interests include power systems and maximum power point tracking (MPPT) for wind energy systems. She can be contacted at khaulahputri@gmail.com.